Efficacy of Tuned Mass Dampers for Bridge Flutter Control

Xinzhong Chen[1] and Ahsan Kareem[2]

Abstract: This paper examines efficacy of tuned mass dampers (TMD) in controlling self-excited motion resulting from negative damping. New optimal TMD parameters are suggested which provide better performance than those suggested in the literature. The dependence of TMD performance on structural damping is highlighted. The equations of motion of a combined system comprised of multiple TMDs attached to a bridge deck are presented where the bridge motion is described in terms of reduced-order modal coordinates. Details concerning the multimode coupled flutter of long-span bridges with auxiliary TMDs are provided. The effectiveness and limitations of TMDs for controlling multimode bridge flutter are examined, emphasizing the dependence of TMD performance on the bridge dynamic and aerodynamic characteristics. This study shows that the effectiveness of TMDs is rather limited in controlling a hard-type flutter characterized by negative aerodynamic damping that grows rapidly with increasing wind speed beyond the onset of flutter. However, it is relatively effective in controlling a soft-type flutter in which the negative damping builds up slowly with increasing wind speed. Robust TMD design issues are also discussed in light of their sensitivity to design parameters in the vicinity of optimal values.

DOI: 10.1061/(ASCE)0733-9445(2003)129:10(1291)

CE Database subject headings: Aerodynamics; Damping; Flutter; Bridges; Wind loads.

Introduction

Flutter instability is of primary concern for wind-resistant design of long-span bridges. The flutter performance of a long-span suspension bridge can be improved through modifications of the structural system such as addition of stay-cables or cross hangers to the original suspension bridge system. These structural modifications result in an increase in not only the structural stiffness, particularly in torsion, but also the generalized modal mass due to three-dimensional mode shapes. The most effective means of flutter control, however, is to improve the aerodynamic performance of a bridge deck section through modifications in its geometric configuration. This helps to control the development of self-excited forces, particularly, it reduces the coupled self-excited forces, i.e., the lift induced by torsional motion and the pitching moment induced by heaving motion.

A number of studies utilizing auxiliary damping devices such as tuned mass dampers (TMDs) or tuned liquid column dampers (TLCDs) have been conducted in controlling bridge flutter (Nobuto et al. 1988; Gu et al. 1998; Lin et al. 2000; Xu et al. 2000). In Nobuto et al. (1988), both numerical analysis and wind tunnel tests of a bridge section model with two TMDs were conducted to demonstrate the effectiveness of TMDs. In Gu et al. (1998), using wind tunnel tests of a box section model, the performance of TMDs with different parameters for controlling flutter was investigated and compared to a numerical study. In Lin et al. (2000), a combination of heaving and torsional dampers was studied to suppress coupled vertical and torsional buffeting response and flutter instability. A TLCD for controlling torsional flutter and buffeting of a long-span bridge was investigated by Xue et al. (2000). The role of modal damping on both flutter and buffeting response of bridges was studied by Jain et al. (1998). For their specific bridge example, slight changes in modal damping resulted in a significant change in response that emphasized the importance of reliable estimates of modal damping for accurate response prediction and the potential advantage of external dampers in controlling bridge response.

While the effectiveness of auxiliary damping in controlling bridge flutter has been demonstrated in foregoing studies for their specific example bridges, its limitation and the dependence of its performance on the bridge structural dynamic and aerodynamic characteristics have not been fully addressed thus far. In this paper, the optimal TMD design for controlling self-excited motions having negative damping is examined. New optimal TMD parameters are proposed which offer better performance than those previously suggested in the literature. The dependence of TMD performance on structural damping is highlighted. The equations of motion for a bridge with multiple TMDs attached to the bridge deck are presented in which the bridge motion is described in terms of reduced-order modal coordinates. Two example long-span bridges with different flutter characteristics are utilized to study the effectiveness and limitations of TMDs in controlling multimode coupled bridge flutter. Emphasis is placed on delineating the dependence of the TMDs performance on the original bridge dynamic and aerodynamic characteristics. Issues related to robust TMD design are also discussed in light of their sensitivity to design parameters around the optimal values.

Tuned Mass Dampers Characteristics in Controlling Self-Excited Motion

To better understand the fundamental characteristics of a TMD in controlling self-excited motion, a single-degree-of-freedom

[1]Postdoctoral Research Associate, Dept. of Civil Engineering and Geological Sciences, Univ. of Notre Dame, Notre Dame, IN 46556. E-mail: xchen@nd.edu

[2]Professor Robert M. Moran, Dept. of Civil Engineering and Geological Sciences, Univ. of Notre Dame, Notre Dame, IN 46556. E-mail: kareem@nd.edu

Note. Associate Editor: Bogusz Bienkiewicz. Discussion open until March 1, 2004. Separate discussions must be submitted for individual papers. To extend the closing date by one month, a written request must be filed with the ASCE Managing Editor. The manuscript for this paper was submitted for review and possible publication on January 12, 2001; approved on January 28, 2003. This paper is part of the ***Journal of Structural Engineering***, Vol. 129, No. 10, October 1, 2003. ©ASCE, ISSN 0733-9445/2003/10-1291–1300/$18.00.

(SDOF) structure with negative net damping combined with a TMD is considered here. The equations of motion of the structure-TMD system are expressed as

$$m_s(\ddot{y}_s+2\xi_s\omega_s\dot{y}_s+\omega_s^2 y_s)=2m_t\xi_t\omega_t(\dot{y}_t-\dot{y}_s)+m_t\omega_t^2(y_t-y_s) \tag{1}$$

$$m_t\ddot{y}_t+2m_t\xi_t\omega_t(\dot{y}_t-\dot{y}_s)+m_t\omega_t^2(y_t-y_s)=0 \tag{2}$$

where m, ξ, and ω = mass, damping ratio, and frequency, respectively; y = displacement; and subscripts s and t represent the structure and TMD, respectively.

By introducing nondimensional time τ and associated derivatives

$$\tau=\omega_s t;\quad \frac{d}{dt}=\omega_s\frac{d}{d\tau};\quad \frac{d^2}{dt}=\omega_s^2\frac{d^2}{d\tau^2} \tag{3}$$

the equations of motion can be expressed in the following nondimensional state-space format:

$$\begin{Bmatrix} y_s' \\ y_t' \\ y_s'' \\ y_t'' \end{Bmatrix} = \begin{bmatrix} 0 & 0 & 1 & 0 \\ 0 & 0 & 0 & 1 \\ -(1+\mu_m\mu_f^2) & \mu_m\mu_f^2 & -2\xi_s-2\mu_m\xi_t\mu_f & 2\mu_m\xi_t\mu_f \\ \mu_f^2 & -\mu_f^2 & 2\xi_t\mu_f & -2\xi_t\mu_f \end{bmatrix} \times \begin{Bmatrix} y_s \\ y_t \\ y_s' \\ y_t' \end{Bmatrix} \tag{4}$$

where $\mu_m=m_t/m_s$ = mass ratio; $\mu_f=\omega_t/\omega_s$ = tuning frequency ratio; and the prime denotes the derivative with respect to the nondimensional time τ. It is clear that the performance of a TMD depends on the mass ratio μ_m, tuning frequency ratio μ_f, TMD damping ratio ξ_t, and structural damping ratio ξ_s.

The eigenvalues of the structure-TMD system can be calculated through the complex eigenvalue analysis based on the preceding state-space equation. For an eigenvalue λ, the characteristic equation of the system described in Eq. (4) is given by

$$\lambda^4+2[\xi_s+(1+\mu_m)\mu_f\xi_t]\lambda^3+[1+(1+\mu_m)\mu_f^2+4\mu_f\xi_s\xi_t]\lambda^2 +2\mu_f[\xi_t+\xi_s\mu_f]\lambda+\mu_f^2=0 \tag{5}$$

When the two conjugate eigenvalue pairs are identical and given by

$$\lambda=a\pm bi=-\xi\omega\pm i\omega\sqrt{1-\xi^2} \tag{6}$$

where ξ and ω = damping ratio and frequency; and $i=\sqrt{-1}$, the characteristic equation reduces to

$$\lambda^4-4a\lambda^3+(6a^2+2b^2)\lambda^2-4a(a^2+b^2)\lambda+(a^2+b^2)=0 \tag{7}$$

For a TMD with a given mass ratio μ_m, the maximum permissible negative damping $(-\xi_s)_{\max}$, under which the structure-TMD system is stable, can be obtained from the condition that the real parts of both eigenvalues of the structure-TMD system are zero, i.e., $\lambda=\pm i\omega$. By comparing the coefficients in Eqs. (5) and (7), and using the condition of zero real part, the following TMD parameters can be obtained, which are generally suggested as the optimal TMD design parameter for controlling self-excited motion (Rowbottom 1981; Fujino and Abe 1993):

$$\mu_f=\frac{1}{\sqrt{1+\mu_m}} \tag{8}$$

$$\xi_t=\sqrt{\frac{\sqrt{1+\mu_m}-1}{2\sqrt{1+\mu_m}}}\approx\sqrt{\mu_m}/2 \tag{9}$$

$$(-\xi_s)_{\max}=\sqrt{\frac{(1+\mu_m)-\sqrt{1+\mu_m}}{2}}\approx\sqrt{\mu_m}/2 \tag{10}$$

However, it is noteworthy that these parameters result in optimal performance only when the negative damping of the self-excited motion is equal to the maximum permissible negative damping $(-\xi_s)_{\max}$ for a given TMD mass ratio. Obviously, this is a very special case. In real TMD design practice for controlling a self-excited motion with a given negative damping ξ_s, the optimal TMD design involves the determination of an adequate mass, optimal frequency, and damping ratio to achieve maximum positive damping available to the structural-TMD system. Changing the negative damping to zero damping only is often not sufficient for motion control. Therefore, the optimal TMD parameters should not be limited to the condition that two identical conjugate eigenvalue pairs have zero real parts. Rather, these should be determined in the general sense as the two identical conjugate eigenvalue pairs reach the maximum of their real parts that correspond to the maximum positive damping. By comparing the coefficients in Eqs. (5) and (7), the optimal TMD parameters become

$$(\mu_f)_{\text{opt}}=\frac{1}{1+\mu_m}-\frac{\sqrt{\mu_m}\xi_s}{(1+\mu_m)\sqrt{1+\mu_m-\xi_s^2}}\approx\frac{1}{1+\mu_m}-\sqrt{\mu_m}\xi_s \tag{11}$$

$$(\xi_t)_{\text{opt}}=\frac{\xi_s}{1+\mu_m}+\frac{\sqrt{\mu_m}\sqrt{1+\mu_m-\xi_s^2}}{1+\mu_m}\approx\frac{\xi_s}{1+\mu_m}+\frac{\sqrt{\mu_m}}{\sqrt{1+\mu_m}} \tag{12}$$

and the identical frequencies and damping ratios are

$$\omega=\sqrt{(\mu_f)_{\text{opt}}} \tag{13}$$

$$\xi=\left(\frac{\xi_s}{1+\mu_m}+\frac{\sqrt{\mu_m}(1+\mu_m-2\xi_s^2)}{2(1+\mu_m)\sqrt{1+\mu_m-\xi_s^2}}\right)/\sqrt{(\mu_f)_{\text{opt}}}\approx\sqrt{\mu_m}/2+\xi_s \tag{14}$$

It can be easily illustrated that for the special case where the mass ratio μ_m and damping ratio ξ_s satisfy the condition $\xi_s=-(-\xi_s)_{\max}$, the optimal parameters given in Eqs. (11) and (12) become the same as those given in Eqs. (8) and (9), corresponding to zero damping ratios of the structural-TMD system.

In the case where ξ_s is small and negligible, by submitting $\xi_s=0$ into Eqs. (11) and (12), these parameters reduce to the following values used in the optimal TMD design for controlling the free vibration:

$$(\mu_f)_{\text{opt}}=1/(1+\mu_m) \tag{15}$$

$$(\xi_t)_{\text{opt}}=\sqrt{\mu_m/(1+\mu_m)} \tag{16}$$

$$\omega=1/\sqrt{1+\mu_m} \tag{17}$$

$$\xi=\sqrt{\mu_m}/2 \tag{18}$$

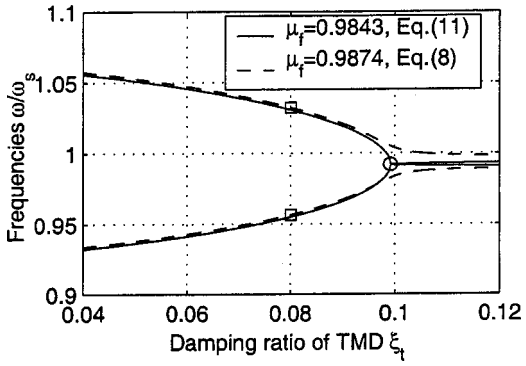

Fig. 1. Frequencies of structure-TMD system ($\mu_m = 0.0256$, $\xi_s = -0.06$)

As an illustrative example, a design of a TMD for controlling a self-excited motion having a negative damping of $\xi_s = -0.06$ with a goal of achieving damping ratios of the structure-TMD system at a level of $\xi = 0.02$ is considered. Based on Eq. (14), the TMD mass ratio is first determined, which should not be less than 0.0256. For $\mu_m = 0.0256$, the optimal tuning frequency ratio is calculated to be $(\mu_f)_{\text{opt}} = 0.9843$ based on Eq. (11). Figs. 1 and 2 show the changes in frequencies and damping ratios of the structure-TMD system with $\mu_m = 0.0256$ and $(\mu_f)_{\text{opt}} = 0.9843$ for different TMD damping ratios as indicated by the solid lines. It is obvious that the optimal TMD damping ratio is $(\xi_t)_{\text{opt}} = 0.0992$ [Eq. (12)], as indicated by the dot in Figs. 1 and 2, corresponding to a damping ratio of $\xi = 0.02$ [Eq. (14)] for the structure-TMD system.

On the other hand, when the TMD is designed based on the formulations previously suggested in the literature [Eqs. (8) and (9)], then $\mu_f = 0.9874$ and $\xi_t = 0.080$. The corresponding frequencies and damping ratios, as indicated by the squares in Figs. 1 and 2, are not identical and suggest a damping ratio of $\xi = 0.0093$ for the structural motion dominated mode. The frequencies and damping ratios of the structure-TMD system with $\mu_m = 0.0256$ and $\mu_f = 0.9874$ and different TMD damping ratios are also shown in Figs. 1 and 2 by the dashed lines. It is obvious that when $\mu_f = 0.9874$, the optimal TMD damping ratio should be $\xi_t = 0.0933$ rather than $\xi_t = 0.080$, corresponding to a damping ratio of $\xi = 0.0123$ for the structure motion dominated mode. Clearly, the TMD design based on the formulations presented here is demonstrably more effective.

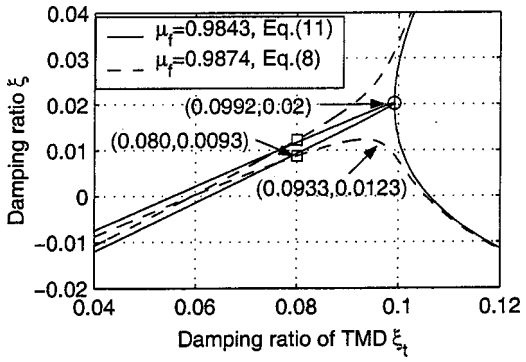

Fig. 2. Damping ratios of structure-TMD system ($\mu_m = 0.0256$, $\xi_s = -0.06$)

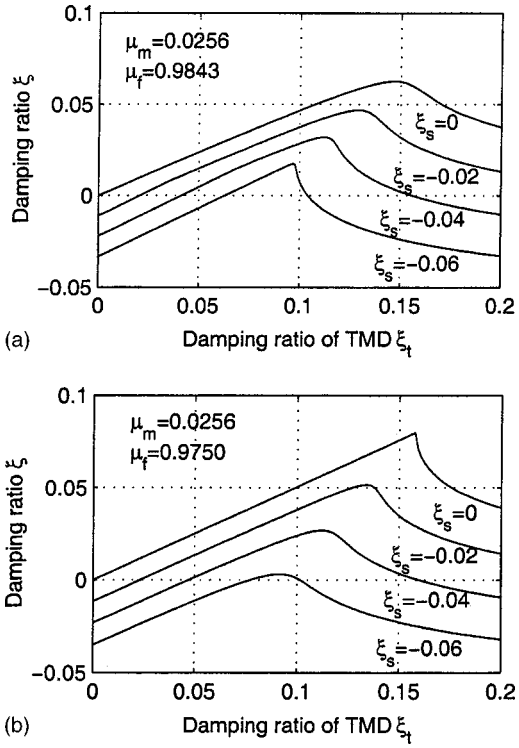

Fig. 3. Influence of structural damping on the performance of TMD ($\mu_m = 0.0256$); (a) $\mu_f = 0.9843$ and (b) $\mu_f = 0.9750$

It is worth mentioning that for a given TMD mass ratio, when the tuning frequency is not aligned with the optimal frequency, the optimal TMD damping ratio should be determined from the eigenvalue analysis of the structure-TMD system including the structural damping. In practice for simplicity, the addition of damping by the TMD is often first evaluated through eigenvalue analysis of the structure-TMD system with zero structural damping, and it is then considered that the structure-TMD system will be stable when the damping added by the TMD is larger than the negative damping caused by the self-excited motion. This practice is based on the premise that the damping added by the TMD is not influenced by the structural damping. This is true when the structural damping is small, but not valid for relative large structural damping as in the case of self-excited motion resulting from a certain level of negative damping. Fig. 3 shows the damping ratio of the structural motion dominated mode at varying levels of original structural damping and TMD damping ratios. It clearly demonstrates the remarkable influence of the original structural damping on the TMD performance in terms of the net damping added by the TMD. This influence is particularly significant for a TMD with a damping ratio close to its optimal value. However, this influence will become less significant when the TMD is designed with higher damping.

As observed in Figs. 2 and 3 and also noted by others, it is reaffirmed that TMD performance is very sensitive to TMD tuning frequency and damping ratio. The robustness of a TMD can be enhanced if multiple tuned mass dampers with distributed frequencies are introduced (Yamaguchi and Harnpornchai 1993; Igusa and Xu 1994; Kareem and Kline 1995), or a TMD with a damping ratio higher than the optimal value is utilized. The latter option, however, will compromise the effectiveness of the TMD. An increase in the mass ratio certainly increases effectiveness, but

not without the adverse effects of higher cost associated with the necessary structural system to support the TMD and the added space requirements.

Multimode Flutter Analysis of Bridge-Tuned Mass Dampers System

A long-span bridge under wind excitation with a number of TMDs attached to the bridge deck is considered. Each TMD is a SDOF system vibrating in the vertical direction. The wind forces on TMDs are assumed to be negligible as the TMDs are considered to be installed inside the bridge box girder. It is assumed that the mass ratio of the TMDs to the equivalent bridge mass is very small, therefore, the attachment of TMDs does not introduce a meaningful change to the static equilibrium of the bridge, and the structural mode shapes remain the same as those of the original bridge without the TMDs. Accordingly, the dynamic displacement of the bridge in the vertical, lateral, and torsional directions $h(x,t)$, $p(x,t)$, and $\alpha(x,t)$ can be expressed in terms of reduced-order modal coordinates as

$$h(x,t)=\sum_j h_j(x)q_j(t); \quad p(x,t)=\sum_j p_j(x)q_j(t);$$

$$\alpha(x,t)=\sum_j \alpha_j(x)q_j(t) \tag{19}$$

where $h_j(x)$, $p_j(x)$, and $\alpha_j(x)=j$th mode shapes of the bridge in the vertical, lateral, and torsional directions, respectively; and $\mathbf{q}=\{q_j\}$=generalized mode coordinates. The positive displacements of vertical, lateral, and torsional components are defined as upward, down-wind, and nose-up, respectively.

The governing equations of motion of the bridge-TMDs system are given by

$$\mathbf{M}\ddot{\mathbf{q}}+\mathbf{C}\dot{\mathbf{q}}+\mathbf{K}\mathbf{q}=\mathbf{Q}_{\text{se}}+\mathbf{Q}_b+\mathbf{Q}_c \tag{20}$$

$$\mathbf{M}_t\ddot{\mathbf{Y}}_t+\mathbf{C}_t(\dot{\mathbf{Y}}_t-\dot{\mathbf{Y}}_0)+\mathbf{K}_t(\mathbf{Y}_t-\mathbf{Y}_0)=\mathbf{0} \tag{21}$$

where $\mathbf{M}$, $\mathbf{C}$, and $\mathbf{K}$=generalized mass, damping, and stiffness matrices of the bridge, respectively; $\mathbf{M}_t$, $\mathbf{C}_t$, and $\mathbf{K}_t$=mass, damping, and stiffness matrices of the TMDs, respectively; $\mathbf{Y}_t$=vertical displacement vector of the TMDs; $\mathbf{Y}_0=\mathbf{B}_t\mathbf{q}$=vertical displacement vector of the bridge deck at the points of attachment of the TMDs; $\mathbf{B}_t$=modal matrix at the points of attachment of TMDs; $\mathbf{Q}_{\text{se}}$ and $\mathbf{Q}_b$=generalized self-excited and buffeting force vectors of the bridge, respectively; and $\mathbf{Q}_c$=control force provided by the TMDs:

$$\mathbf{Q}_c=\mathbf{B}_t^T\mathbf{C}_t(\dot{\mathbf{Y}}_t-\dot{\mathbf{Y}}_0)+\mathbf{B}_t^T\mathbf{K}_t(\mathbf{Y}_t-\mathbf{Y}_0) \tag{22}$$

the over-dot denotes partial differentiation with respect to time; and superscript T denotes the matrix transpose operator.

The frequency dependent self-excited forces can be replaced by a rational function approximation as (Chen et al. 2000)

$$\mathbf{Q}_{\text{se}}=\frac{1}{2}\rho U^2\left(\mathbf{A}_s\mathbf{q}+\frac{b}{U}\mathbf{A}_d\dot{\mathbf{q}}\right)$$

$$=\frac{1}{2}\rho U^2\left(\mathbf{A}_1\mathbf{q}+\frac{b}{U}\mathbf{A}_2\dot{\mathbf{q}}+\frac{b^2}{U^2}\mathbf{A}_3\ddot{\mathbf{q}}+\sum_{l=1}^{m}\mathbf{q}_{\text{sel}}\right) \tag{23}$$

where

$$\dot{\mathbf{q}}_{\text{sel}}=-\frac{Ud_l}{b}\mathbf{q}_{\text{sel}}+\mathbf{A}_{l+3}\dot{\mathbf{q}} \quad (l=1,2,...,m) \tag{24}$$

and $\mathbf{A}_s$ and $\mathbf{A}_d$=aerodynamic stiffness and damping matrices, respectively; $\mathbf{A}_1$, $\mathbf{A}_2$, $\mathbf{A}_3$, $\mathbf{A}_{l+3}$, and d_l ($d_l\geqslant 0$; $l=1,2,...,m$)=frequency independent coefficients; $\mathbf{q}_{\text{sel}}$ ($l=1,2,...,m$)=augmented unsteady aerodynamic states; m=order of the rational function approximation; ρ=air density; $B=2b$=width of the bridge deck; and U=mean wind speed.

Accordingly, the equations of motion of the bridge-TMDs system can be cast in terms of a frequency independent time-invariant state-space format

$$\dot{\mathbf{Z}}(t)=\mathbf{A}\mathbf{Z}(t)+\mathbf{B}\mathbf{Q}_b(t) \tag{25}$$

where

$$\mathbf{Z}=\begin{Bmatrix}\mathbf{q}\\ \mathbf{Y}_t\\ \dot{\mathbf{q}}\\ \dot{\mathbf{Y}}_t\\ \mathbf{q}_{\text{sel}}\\ \vdots\\ \mathbf{q}_{\text{sem}}\end{Bmatrix}; \quad \mathbf{B}=\begin{bmatrix}\mathbf{0}\\ \mathbf{0}\\ \tilde{\mathbf{M}}^{-1}\\ \mathbf{0}\\ \mathbf{0}\\ \vdots\\ \mathbf{0}\end{bmatrix} \tag{26}$$

$$\mathbf{A}=\begin{bmatrix}
\mathbf{0} & \mathbf{0} & \mathbf{I} & \mathbf{0} & \mathbf{0} & \cdots & \mathbf{0}\\
\mathbf{0} & \mathbf{0} & \mathbf{0} & \mathbf{I} & \mathbf{0} & \cdots & \mathbf{0}\\
-\overline{\mathbf{M}}^{-1}(\overline{\mathbf{K}}+\mathbf{B}_t^T\mathbf{K}_t\mathbf{B}_t) & \overline{\mathbf{M}}^{-1}\mathbf{B}_t^T\mathbf{K}_t & -\overline{\mathbf{M}}^{-1}(\overline{\mathbf{C}}+\mathbf{B}_t^T\mathbf{C}_t\mathbf{B}_t) & \overline{\mathbf{M}}^{-1}\mathbf{B}_t^T\mathbf{C}_t & \frac{1}{2}\rho U^2\overline{\mathbf{M}}^{-1} & \cdots & \frac{1}{2}\rho U^2\overline{\mathbf{M}}^{-1}\\
\mathbf{M}_t^{-1}\mathbf{K}_t\mathbf{B}_t & -\mathbf{M}_t^{-1}\mathbf{K}_t & \mathbf{M}_t^{-1}\mathbf{C}_t\mathbf{B}_t & -\mathbf{M}_t^{-1}\mathbf{C}_t & \mathbf{0} & \cdots & \mathbf{0}\\
\mathbf{0} & \mathbf{0} & \mathbf{A}_4 & \mathbf{0} & -\frac{U}{b}d_1\mathbf{I} & \cdots & \mathbf{0}\\
\vdots & \vdots & \vdots & & \vdots & & \\
\mathbf{0} & \mathbf{0} & \mathbf{A}_{3+m} & \mathbf{0} & \mathbf{0} & \cdots & -\frac{U}{b}d_m\mathbf{I}
\end{bmatrix} \tag{27}$$

$$\overline{\mathbf{M}}=\mathbf{M}-\frac{1}{2}\rho b^2\mathbf{A}_3;\quad \overline{\mathbf{C}}=\mathbf{C}-\frac{1}{2}\rho Ub\mathbf{A}_2;\quad \overline{\mathbf{K}}=\mathbf{K}-\frac{1}{2}\rho U^2\mathbf{A}_1 \tag{28}$$

At a given wind speed U, the solution of a linear complex eigenvalue problem given by

$$\lambda_j\mathbf{\Phi}_j=\mathbf{A}\mathbf{\Phi}_j \tag{29}$$

results in $N+M$ conjugate pairs of complex eigenvalues and eigenvectors (where N is the number of structural modes included and M is the number of TMDs), and $m\times N$ negative real eigenvalues and real eigenvectors. The former group of eigenvalues corresponds to the modes associated with the bridge-TMD system, and the latter represent the augmented aerodynamic states introduced by the rational function approximation of the self-excited forces. These complex modes are referred to as ''mode branches.''

The eigenvalue of the jth complex mode is expressed as

$$\lambda_j=-\xi_j\omega_j+i\omega_j\sqrt{1-\xi_j^2} \tag{30}$$

where ω_j and ξ_j = mode frequency and damping ratio.

These eigenvalues at different wind speeds provide information concerning the changes in frequencies, damping ratios that take place with the increase in wind speed. The system is stable when all of the eigenvalues lie on the left side of the imaginary axis in the complex plane. When one of the eigenvalues has a zero real part, it represents the onset of flutter and the corresponding wind speed is referred to as the critical flutter speed.

The corresponding eigenvectors $\mathbf{\Phi}_j$ ($j=1,2,...,$) provide information concerning intermodal coupling among the structural modes, and the coupling between the bridge motion and motion of the attached TMDs with phase lags. The preceding formulation reduces to the multimode flutter analysis of the bridge without TMDs by dropping the terms with respect to the TMDs.

It is noted that the framework presented in this study, where the bridge motion is expressed in terms of reduced-order structural mode coordinates, provides a straightforward relationship regarding the influence of installed TMDs on the structural dynamics/aerodynamics as compared to the analysis based on a direct finite element model of the bridge-TMDs system.

Example Bridges

Two example long-span suspension bridges, i.e., Bridges A and B, with same structural dynamics but different aerodynamic characteristics are considered to illustrate the effectiveness and limitations of TMDs in controlling bridge flutter. The length of the bridge main span is nearly 2,000 m. The modal frequencies of the first 15 modes range from 0.03 to 0.18 Hz. The structural modal damping ratio in each mode is assumed to be the same and equal to 0.32% for the sake of illustration. The selection of this damping ratio is based on the value for long-span bridges having box girders, which has been suggested by the Honshu-Shikoku Bridge wind resistant design code in Japan (Miyata et al. 1993). The modal damping ratios for different structural modes are generally different. The influence of structural modal damping on bridge flutter will be further highlighted in the following.

Bridge A has a streamlined deck section whose flutter derivatives are calculated based on the Theodorsen function. Bridge B has a 2-edge box deck section whose flutter derivatives are determined through a wind tunnel test (Matsumoto et al. 1998). Some of their representative flutter derivatives are presented in Fig. 4, including uncoupled torsional damping and stiffness terms, A_2^* and A_3^* and coupled terms, H_3^* and A_1^*. The solid lines represent those for Bridge A and the dashed lines for Bridge B. The definition of flutter derivatives and a detailed discussion on the role of each aerodynamic component on coupled flutter can be found in Chen et al. (2000). In the following multimode bridge flutter analysis, only the self-excited forces acting on the bridge deck which dominate the bridge flutter are considered. The secondary contributions of aerodynamic damping on the main cables, hanger cables, and towers are neglected for the sake of illustration.

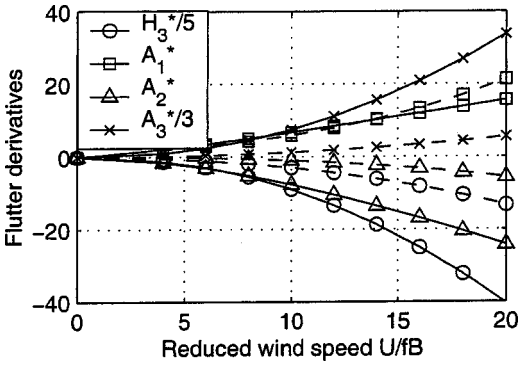

Fig. 4. Flutter derivatives of bridge decks (—Bridge A: --Bridge B)

Flutter Response

The multimode coupled flutter analyses involving different combination of structural modes for both Bridges A and B suggested that a consideration of only a few important structural modes can provide an accurate estimate of flutter response. Therefore, the following discussion is based on the analyses considering only the first and second symmetric vertical bending modes (Modes 2 and 8) and the first symmetric torsional mode (Mode 10).

The changes in frequencies and damping ratios with increasing wind speed for Bridge A are shown in Figs. 5 and 6 by dots. The damping ratios are expressed in terms of logarithmic decrement, i.e., $\delta=2\pi\xi$. With an increase in the mean wind speed, the corresponding mode shapes vary with wind speed from real-valued structural mode shapes at zero wind speed to complex-valued shapes at higher wind speeds, indicating intermode coupling due to self-excited aerodynamic forces. The coupled flutter initiates from the Mode 10 branch with a critical wind speed of 67.7 m/s. Table 1 shows the flutter frequency and mode shape in terms of

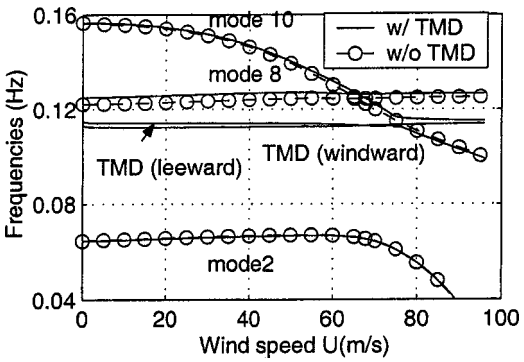

Fig. 5. Frequencies versus wind speed for Bridge A

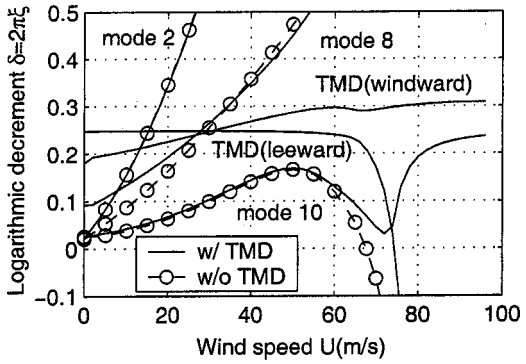

Fig. 6. Damping ratios versus wind speed for Bridge A

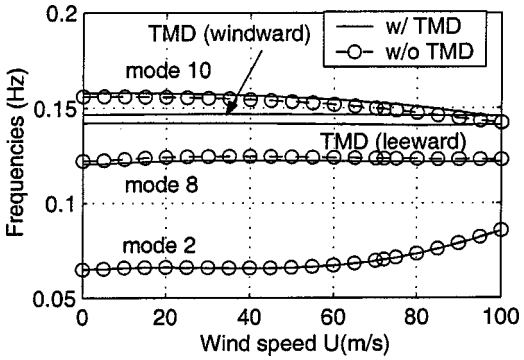

Fig. 7. Frequencies versus wind speed for Bridge B

the amplitude ratios and phase lags of components in each structural mode. It is noted that the structural mode shapes were normalized according to the maximum vertical displacement or torsional displacement multiplied by the half width of the bridge deck to be unity for the vertical or torsional modes, respectively. The vertical displacements of the bridge deck on the windward and leeward sides at Points A and B located at $0.75b$ (b is the half-width of the bridge deck) from the deck centerline at the midspan of the bridge are also calculated and presented in Table 1. It is clearly demonstrated that the torsional displacement lags downward vertical displacement, and the vertical displacement of the bridge deck at the leeward side is larger than that at windward side. The flutter of Bridge A corresponds to a hard-type flutter characterized by negative aerodynamic damping that grows rapidly with increasing wind speed beyond the onset of flutter.

The results for Bridge B with the modal damping ratio of 0.32% are shown in Figs. 7 and 8 and Table 2. The predicted critical flutter speed for Bridge B is 72.0 m/s. As compared to Bridge A, in which significant coupling between bridge motion in vertical and torsional directions was observed, the coupled motion in Bridge B is relatively weak but remains essential to the development of coupled flutter initiated from Mode 10 branch. From the flutter derivative A_2^*, which shows a negative value, it is obvious that the aeroelastic damping of torsional Mode 10 without coupling with the vertical modes would have remained positive and thus a single mode flutter would not exist. While the torsional aerodynamic damping term (corresponding to A_2^*) is remarkably low compared to that of Bridge A, a significant decrease in the coupled self-excited forces resulted in lowering the negative damping effects thus producing a better flutter performance of Bridge B. The flutter of Bridge B corresponds to a soft-type flutter in which the negative damping builds up slowly with increasing wind speed.

Influence of Structural Damping on Bridge Flutter

To investigate the effect of structural damping on the flutter response, an analysis with different modal damping ratios has been conducted for both Bridges A and B. These include the analysis in which different modal damping ratios for different modes were assigned and identical damping ratios for each mode with assigned values of 0.0, 0.32, 1, and 2% were assumed.

Results illustrated that the influence of low structural modal damping on the frequency, aerodynamic damping, and complex mode shapes is negligible. Total aeroelastic modal damping can be simply estimated as the sum of structural modal damping and the aerodynamic damping estimated with zero structural damping. The critical flutter speeds for Bridge A having structural modal damping ratios of 0.0, 0.32, 1, and 2% are 66.0, 67.7, 69.7, and 72.2 m/s, respectively. The effect of structural modal damping on the critical flutter speed is rather insignificant for this bridge. This is because the negative damping grows rapidly with increasing wind speed beyond the flutter onset and the addition of damping does not result in an apparent increase in the critical flutter speed.

The critical flutter speeds for Bridge B with structural damping ratios of 0, 0.32, 1, and 2% are 63.9, 72.0, 80.7, and 88.0 m/s, respectively. Due to the weak coupled self-excited forces and the lower torsional aerodynamic damping, the development of aeroelastic damping in the torsional mode branch is rather slow

Table 1. Comparison of Flutter Condition for Bridge A

	Without tuned mass dampers		With tuned mass dampers[a]
Wind speed	67.7 m/s	74.5 m/s	74.5 m/s
Frequency	0.1223 Hz	0.1155 Hz	0.1133 Hz
Damping ratio	0	−0.0349	0
Mode number	Amplitude/Phase (degrees)	Amplitude/Phase (degrees)	Amplitude/Phase (degrees)
Mode 2	1.21/−162.78	1.70/−154.04	1.74/−156.13
Mode 8	0.64/−76.83	0.52/−60.90	0.36/2.00
Mode 10	1.00/0	1.00/0	1.00/0
Point A (windward)	1.02/−104.84	1.31/−113.68	0.84/−124.84
Point B (leeward)	2.02/−150.86	2.35/−149.39	2.10/−160.76
Tuned mass dampers (windward)	—/—	—/—	9.99/166.27
Tuned mass dampers (leeward)	—/—	—/—	24.82/130.73

[a] $\mu_t = 175$ t, $f_t = 0.1147$ Hz, $\xi_t = 0.04$

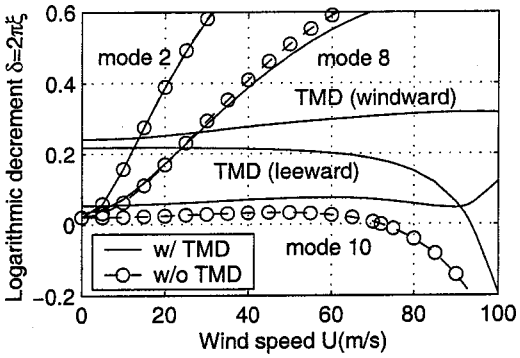

Fig. 8. Damping ratios versus wind speed for Bridge B

with increasing wind speed. Accordingly, the critical flutter speed can be significantly increased by the addition of auxiliary damping. Similar to the example bridge studied by Jain et al. (1998), slight changes in modal damping will result in significantly different response which emphasized the importance of reliable estimates of modal damping for accurate prediction of response.

Control of Bridge Flutter by Tuned Mass Dampers

For the sake of illustration, only two TMDs with the same parameters vibrating in vertical direction were considered. They were installed on the windward and leeward sides at Points A and B located at $0.75b$ from the deck centerline at the midspan of the bridge. The TMDs are designed to control the initial coupled flutter having coupled bridge motion mainly attributed to the symmetric structural modes. It is noted that such TMDs will have little contribution to controlling any subsequent bridge flutter modes due to the lack of tuning and/or improper placement of the TMDs. To suppress these higher flutter modes, a properly designed TMD configuration is required based on the frequency, damping ratio, and mode shape of each target flutter mode on the lines of the TMD design for the initial flutter mode. This issue is beyond the focus of this study and is therefore not further addressed.

The mass was set as $m_t=175$ t for each individual TMD. Therefore, the equivalent mass ratio of the TMDs to the first symmetric vertical mode, i.e., Mode 2, is $2m_t h_2^2(x)|_{x=L/2}/m_2=0.57\%$, and the mass of inertia ratio of the TMDs to the first symmetric torsional mode, i.e., Mode 10, is $2m_t[0.75b\alpha_{10}^2(x)|_{x=L/2}]/m_{10}=0.58\%$, where m_2 and m_{10} are the generalized mass in Modes 2 and 10, respectively. In practical TMD design, multiple TMDs each comprised of a smaller mass with the same or slightly detuned dynamic properties can be installed at different spanwise locations with consideration of space limitation. In this study, since the emphasis is placed on the dependence of TMD performance on the bridge aerodynamic characteristics, a relatively simple TMD design configuration is considered.

Based on the dynamic characteristics of Bridge A, the TMDs were designed to control Mode Branch 10 from which the coupled flutter is initiated. Utilizing Eqs. (11) and (12), the TMD tuning frequency ratio and damping ratio are 0.9972 and 0.0533 for $\mu_m=0.29\%$ and $\xi_s=0$. However, the optimal TMD parameters for controlling a coupled flutter could not be directly determined based on explicit formulations for controlling a SDOF self-excited motion. It is due to the fact that the frequency, damping ratio, and the complex mode shape of the target mode branch vary with increasing wind speed, which affects the performance of a TMD. A better TMD design can be achieved through parametric studies involving eigenvalue analysis of the bridge-TMDs system at different wind speed. In this study, the frequency and damping ratio of the TMDs were initially set as $f_t=0.1159$ Hz and $\xi_t=0.04$, respectively.

The frequencies and damping ratios of the Bridge A-TMD system are plotted versus the mean wind speed in Figs. 5 and 6 as indicated by the solid lines. At low wind speeds, since the natural frequencies of TMDs are separated from the frequencies of Mode Branches 2 and 10 but are relatively close to the frequency of Mode Branch 8, only the damping ratio associated with the Mode Branch 8 is slightly influenced by the inclusion of the TMDs. At a wind speed of around 74 m/s, due to the interaction between Mode Branch 10 and the TMDs, particularly the TMD on the leeward side, the damping in Mode Branch 10 increases and damping in the TMD dominated mode branch decreases. The curves of two frequency loci representing Mode Branch 10 and leeward TMD branch repel each other thus avoiding an intersection. As a result, the coupled flutter initiates from the leeward TMD branch. In this strong interaction region, two branches exhibit coupled motions of the bridge and TMDs. Although the curve veers, the properties of these two mode branches interchange during the veering, and the curve veering phenomenon is observed in this interaction region. The curve veering phenomenon is widely observed in multimode coupled flutter problems and other dynamic problems. A detailed discussion of this phenomenon, including the criterion for identification of veering, has been discussed using a perturbation analysis in Chen and Kareem

Table 2. Comparison of Flutter Condition for Bridge B

	Without tuned mass dampers		With tuned mass dampers[a]
Wind speed	72.0 m/s	94.7 m/s	94.7 m/s
Frequency	0.1495 Hz	0.1435 Hz	0.1413 Hz
Damping ratio	0	−0.0347	0
Mode number	Amplitude/Phase (degrees)	Amplitude/Phase (degrees)	Amplitude/Phase (degrees)
Mode 2	0.27/175.03	0.57/177.78	0.55/175.07
Mode 8	0.11/−167.48	0.21/−151.97	0.14/−98.62
Mode 10	1.00/0	1.00/0	1.00/0
Point A (windward)	0.37/−0.07	0.08/−93.69	0.20/153.27
Point B (leeward)	1.13/−179.98	1.51/−177.09	1.32/−176.04
Tuned mass dampers (windward)	—/—	—/—	2.42/−93.73
Tuned mass dampers (leeward)	—/—	—/—	15.86/177.17

[a]$\mu_m=175$ t, $f_t=0.1433$ Hz, $\xi_t=0.04$.

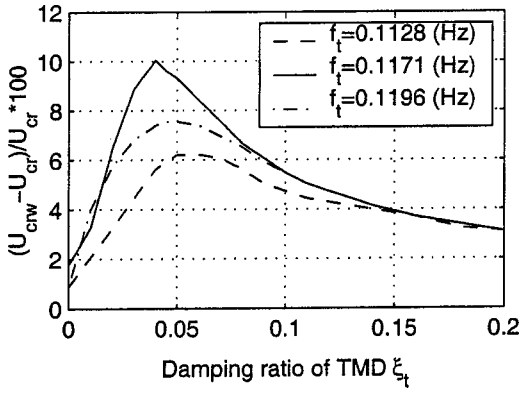

Fig. 9. Effectiveness of TMDs versus damping ratio of TMD for Bridge A

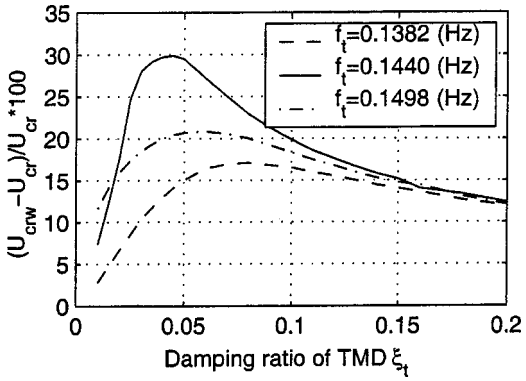

Fig. 11. Effectiveness of TMDs versus damping ratio of TMD for Bridge B

(2003). Beyond this strong interaction region, the flutter mode branch mainly consists of bridge motions and only slightly involves the motions of TMDs.

Table 1 shows the flutter frequency and mode shape of the Bridge A-TMDs system in terms of the amplitude ratios and phase lags of the components in each structural mode, the vertical displacements of the bridge deck at the Points A and B where the TMDs were attached, and the displacements of the TMDs. For comparison, the results of the bridge without TMDs at 74.5 m/s are also presented. It is illustrated that the addition of TMDs does not significantly change the coupled motion of the bridge, which is due to self-excited aerodynamic forces on the bridge. The attached TMDs experience large amplitude of motions, particularly, the leeward side TMD compared to the windward side TMD. However, two TMDs show similar dynamic responses with regard to the respective displacements of the bridge deck. The amplitude ratios and phase lags of the TMDs displacements with respect to the downward displacements of the bridge deck at Points A and B are almost the same for the two TMDs, which are around 11.8 and 68.5°. It is not surprising that the stabilization role of the TMDs is mainly due to the leeward side TMD corresponding to a larger bridge deck excitation at the Point B. As a result, the critical flutter speed is increased to 74.5 m/s from 67.7 m/s with the addition of the TMDs.

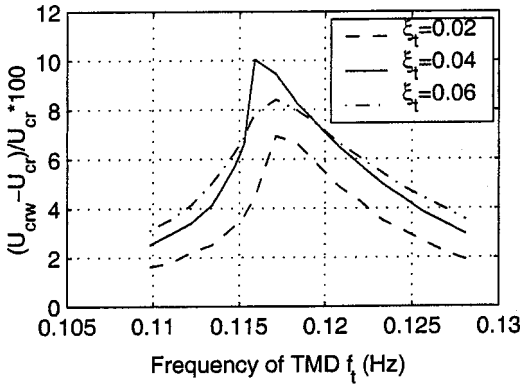

Fig. 10. Effectiveness of TMDs versus frequency of TMD for Bridge A

Figs. 9 and 10 show the effectiveness of TMDs expressed in terms of increase ratio of the critical flutter speed due to the addition of the TMDs, i.e., $(U_{\mathrm{crw}}-U_{\mathrm{cr}})/U_{\mathrm{cr}}$, with different TMD tuning frequencies and damping ratios, where the U_{crw} and U_{cr} are the critical flutter speed with and without TMDs. The optimal parameters are about $f_t=0.1171$ Hz and $\xi_t=0.04$. Similar to the TMD characteristics in controlling a SDOF self-excited motion, the TMD performance in controlling a multimode coupled flutter is sensitive to their own dynamic parameters, particularly, their frequencies. Optimal TMD design in controlling bridge flutter requires an accurate estimate of the torsional mode branch frequency. For long-span bridges with low fundamental frequencies, it may be very difficult to design a robust set of TMDs due to a high sensitivity of the TMD effectiveness around optimal parameters. The design of TMDs with a damping ratio higher than the optimal value may add to the robustness, but not without some compromise on the overall effectiveness.

Since the coupled self-excited forces result in a rapid increase in negative aerodynamic damping at higher wind speeds for Bridge A, the addition of damping provided by TMDs does not result in an appreciable change in the critical flutter speed. For this hard-type of flutter, the addition of auxiliary damping contributes only marginally toward controlling the flutter instability.

The changes in frequencies and damping ratios for Bridge B with TMDs at increasing wind speeds are shown in Figs. 7 and 8 as indicated by the solid lines. The frequency and damping ratio of the TMDs were set as $f_t=0.1433$ Hz and $\xi_t=0.04$. The critical flutter speed is increased from 72.0 to 94.7 m/s. The TMD appears to be very efficient in controlling this soft-type flutter of Bridge B. However, similar to the case of Bridge A, the TMD performance strongly depends on the TMD tuning frequency and damping ratio as noted in Figs. 11 and 12.

Table 2 summarizes the flutter frequency and mode shape of the Bridge B-TMDs system in terms of the amplitude ratios and phase lags of the components in each structural mode, the vertical displacements of the bridge deck at Points A and B where the TMDs were attached, and the displacements of the TMDs. For comparison, the results of Bridge A without TMDs at 94.7 m/s are also presented. Similar to the case of Bridge A, it is reaffirmed that two TMDs show similar dynamic responses with regard to the respective displacements of the bridge deck. The amplitude ratio and phase lags of TMD with respect to the deck displacement are almost the same for the two TMDs, which are around 11.9 and 66.8°. The leeward side TMD plays an essential role in controlling the bridge flutter.

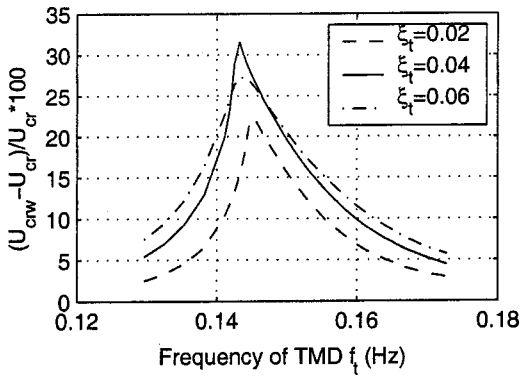

Fig. 12. Effectiveness of TMDs versus frequency of TMD for Bridge B

The TMD stroke has been a major constraint in TMD design along with the TMD mass. The information concerning the displacements of the TMDs with respect to the displacement of the bridge deck in the flutter mode provided in Tables 1 and 2 helps to clarify this important issue.

Concluding Remarks

Optimal TMD design in controlling self-excited motion resulting from a given negative damping was examined with a goal of achieving a target positive damping, and a new set of expressions for the optimal TMD parameters was presented. It was illustrated that the optimal design parameters suggested in the literature result in an optimal performance only when the resulting damping ratios of the structure-TMD system are identical and equal to zero. The optimal TMD design suggested by the present study offers a better performance. It was emphasized that the TMD performance may be remarkably influenced by structural damping as in the case of self-excited motion with a certain level of negative damping.

A low structural damping value has negligible influence on the aeroelastic modal characteristics of bridges, i.e., frequency, aerodynamic damping and complex mode shapes. Total aeroelastic modal damping can be simply estimated as the sum of structural modal damping and the aerodynamic damping estimated with zero structural damping.

A detailed discussion of the eigenvalues of the bridge-TMDs system and the intermodal coupling among structural modes and coupling between bridge and TMDs was provided using example bridges. The complex eigenvalue analysis of bridge-TMDs system provided essential information concerning the bridge-TMDs interaction. The displacements of the TMDs with respect to the bridge deck in the flutter mode helped to clarify the issue of TMD stroke which has been a main constraint in TMD design along with the TMD mass.

It was illustrated that the addition of TMDs did not significantly change the coupled motion of the bridge, which was due to self-excited aerodynamic forces on the bridge. The attached TMDs experienced large amplitude motions, particularly, the leeward side TMD as compared to the windward side. However, both side TMDs showed similar dynamic responses with regard to the respective displacements of the bridge deck. The stabilizing role of TMDs was mainly due to the leeward side TMD which corresponded to a larger bridge deck excitation as compared to those at windward side.

While the effectiveness of auxiliary dampers in controlling bridge flutter has been demonstrated in foregoing studies for their specific example bridges, their limitation and the dependence of their performance on the original structural dynamic and aerodynamic characteristics have not been fully addressed thus far in the literature. This study showed that the performance of TMDs strongly depends on the bridge aerodynamic characteristics. For a hard-type flutter characterized by negative damping that grows rapidly with increasing wind speed beyond the flutter onset, the influence of structural modal damping on the critical flutter speed was insignificant. Accordingly, the effectiveness of TMDs in controlling this type of flutter was rather marginal. However, for a soft-type flutter in which the negative damping of bridges grows slowly with increasing wind speed, addition of auxiliary damping may result in significantly higher flutter speed. For this type of flutter, a reliable estimate of structural modal damping was critical for accurate estimation of flutter, and auxiliary dampers such as TMDs would be relatively effective in controlling flutter.

From a practical viewpoint, in addition to the need to provide a support system and the space needed for the housing of TMDs with large dynamic displacements, it may be very difficult to configure robust TMDs in light of the sensitivity of their performance to design parameters around their optimal values for long-span bridges with very low frequencies. It is emphasized that for controlling flutter instability, instead of adding indirect damping to the bridge system through the use of TMDs or even active control devices, attention must be focused on controlling the development of self-excited aerodynamic forces through passive and/or active aerodynamic control schemes. A proper combination involving modification of aerodynamic characteristics to allow a hard-type flutter to become a soft-type flutter and addition of auxiliary damping devices may offer an effective solution for bridge flutter control.

Acknowledgments

The support for this work was provided in part by NSF Grant Nos. CMS 9402196 and CMS 95-03779. This support is gratefully acknowledged. The writers are thankful to Dr. Fred Haan, Jr., visiting assistant professor in the Department of Civil Engineering and Geological Sciences, University of Notre Dame, Notre Dame, Ind., for his comments on the manuscript.

References

Chen, X., and Kareem, A. (2003). ''Curve veering of eigenvalue loci of bridges with aeroelastic effects.'' *J. Eng. Mech.*, 129(2), 146–159.

Chen, X., Matsumoto, M., and Kareem, A. (2000). ''Aerodynamic coupling effects on flutter and buffeting of bridges.'' *J. Eng. Mech.*, 126(1), 17–26.

Fujino, Y., and Abe, M. (1993). ''Design formulas for tuned mass dampers based on a perturbation technique.'' *Earthquake Eng. Struct. Dyn.*, 22, 833–854.

Gu, M., Chang, C. C., Wu, W., and Xiang, H. F. (1998). ''Increase of critical flutter wind speed of long-span bridges using tuned mass dampers.'' *J. Wind. Eng. Ind. Aerodyn.*, 73, 111–123.

Igusa, T., and Xu, K. (1994). ''Vibration control using multiple tuned mass dampers.'' *J. Sound Vib.*, 175(4), 491–503.

Jain, A., Jones, N. P., and Scanlan, R. H. (1998). ''Effect of modal damping on bridge aeroelasticity.'' *J. Wind. Eng. Ind. Aerodyn.*, 77 and 78, 421–430.

Kareem, A., and Kline, S. (1995). ''Performance of multiple mass dampers under random loading.'' *J. Struct. Eng.*, 121(2), 348–361.

Lin, Y.-Y., Cheng, C.-M., and Lee, C.-H. (2000). ''A tuned mass damper for suppressing the coupled flexural and torsional buffeting response of long-span bridges.'' *Eng. Struct.*, 22, 1195–1204.

Matsumoto, M., Yagi, T., Ishizaki, H., Shirato, H., and Chen, X. (1998). ''Aerodynamic stability of 2-edge girders for cable-stayed bridge.'' *Proc., 15th National Symp. on Wind Engineering*, Japan Association for Wind Engineering (JAWE), 389–394 (in Japanese).

Miyata, T., Tada, K., and Katsuchi, H. (1993). ''Wind resistant design considerations for the Akashi Kaikyo Bridge.'' *Int. Seminar on Utilization of Large Boundary Layer Wind Tunnel*, Public Works Research Institute, Ministry of Construction, Tsukuba, Japan, 79–100.

Nobuto, J., Fujino, Y., and Ito, M. (1988). ''A study on the effectiveness of TMD to suppress a coupled flutter of bridge deck.'' *Proc. JSCE*, 398/I-10, 413–416.

Rowbottom, M. D. (1981). ''The optimization of mechanical dampers to control self-excited galloping oscillations.'' *J. Sound Vib.*, 75(4), 559–576.

Xue, S. D., Ko, J. M., and Xu, Y. L. (2000). ''Control of torsional flutter and buffeting of long span bridges using liquid column damper.'' *Proc., Int. Conf. on Advances in Structural Dynamics*, December, Hong Kong, J. M. Ko and Y. L. Xu, eds., Elsevier, Oxford, U. K., 1413–1420.

Yamaguchi, H., and Harnpornchai, N. (1993). ''Fundamental characteristics of multiple tuned mass dampers for suppressing harmonically forced oscillations.'' *Earthquake Eng. Struct. Dyn.*, 22, 51–62.